# P-type conductive amorphous oxides of transition metals from solution processing

Jinwang Li, Toshihiko Kaneda, Eisuke Tokumitsu, Mikio Koyano, Tadaoki Mitani et al.

Citation: Appl. Phys. Lett. **101**, 052102 (2012); doi: 10.1063/1.4739936
View online: http://dx.doi.org/10.1063/1.4739936
View Table of Contents: http://apl.aip.org/resource/1/APPLAB/v101/i5
Published by the American Institute of Physics.

# P-type conductive amorphous oxides of transition metals from solution processing

Jinwang Li (李 金望),[1,2,a)] Toshihiko Kaneda (金田 敏彦),[1]
Eisuke Tokumitsu (徳光 永輔),[1,2,3,4] Mikio Koyano (小矢野 幹夫),[2,3]
Tadaoki Mitani (三谷 忠興),[1] and Tatsuya Shimoda (下田 達也)[1,2,3]
[1]*Japan Science and Technology Agency (JST), ERATO, Shimoda Nano-Liquid Process Project, 2-5-3 Asahidai, Nomi, Ishikawa 923-1211, Japan*
[2]*Green Devices Research Center, Japan Advanced Institute of Science and Technology, 1-1 Asahidai, Nomi, Ishikawa 923-1292, Japan*
[3]*School of Materials Science, Japan Advanced Institute of Science and Technology, 1-1 Asahidai, Nomi, Ishikawa 923-1292, Japan*
[4]*Precision and Intelligence Laboratory, Tokyo Institute of Technology, 4259-R2-19 Nagatsuta, Midori-ku, Yokohama 226-8503, Japan*

(Received 16 March 2012; accepted 13 July 2012; published online 30 July 2012)

We report a series of solution-processed p-type conductive amorphous Ln-M-O (a-Ln-M-O, where M = Ru, Ir, and Ln is a lanthanide element except Ce) having low resistivities ($10^{-3}$ to $10^{-2}\,\Omega\,cm$). These oxides are thermally stable to a high degree, being amorphous up to 800 °C, and processable below 400 °C. Their film surfaces are smooth on the atomic scale, and the process allows patterning simply by direct imprinting without distortion of the pattern after annealing. These properties have high potential for use in printed electronics. The electron configurations of these oxides are apparently different from existing p-type oxides. © *2012 American Institute of Physics*. [http://dx.doi.org/10.1063/1.4739936]

Printing techniques for electronic devices are intensively studied because of their low-energy input and applicability to large-area substrates.[1] In particular, printed devices composed of only oxides are attractive for vacuum-free "green production" of electronics in the future, because oxides are processable in ambient atmosphere, unlike silicon, and are thermally stable compared to organics. Furthermore, the use of amorphous oxides (a-oxides) is extremely important because of their merits over crystalline materials: deposits are uniform over a large area; film surfaces are flat; films are free of vulnerable boundaries; low-processing temperatures, which are compatible with low-cost substrates, can be used; etc. Especially, for nanodevices, size scaling down is restricted by the crystal size (typically over 20 nm) in case of polycrystalline materials, and thus amorphous materials are indispensable. To realize all-amorphous oxide electronics by printing, functional a-oxides (conductors, semiconductors and dielectrics) have to be solution-processed. Although there are some examples of a-oxide dielectrics[2,3] and n-type semiconductors[4–8] using solution methods, efforts in this field regarding a-oxides for electrode and p-type channel applications have been in vain. In fact, research towards p-type a-oxides is highly challenging even by using vacuum deposition techniques, which results in only two materials: Zn-Rh-O (resistivity $\sim 0.5\,\Omega\,cm$)[9,10] and Zn-Co-O ($\sim 0.05\,\Omega\,cm$).[11]

Breakthrough research toward p-type oxides has been performed by the Hosono group, who performed pioneering studied on both n- and p-type oxide semiconductors.[9,10,12–19] It is known that p-type oxides are rare, while n-type oxides are common. In searching p-type oxides, they found a series of transparent p-type Cu oxides with delafossite structure.[16,17] However, the amorphous phases of these oxides did not show p-type conduction, which was attributed to the failure in maintaining the same local structure as in the crystalline phases.[9,10] They then studied the Zn-Rh-O system and obtained the first p-type a-oxide, which maintained the same edge-sharing $RhO_6$ network as in the p-type $ZnRh_2O_4$ crystals.[9,10] Later, another p-type a-oxide, Zn-Co-O, was produced.[11] All these oxides were produced by vacuum deposition techniques.

Here we report a series of solution-processed p-type conductive amorphous Ln-M-O (a-Ln-M-O, where M = Ru, Ir, and Ln is a lanthanide element except Ce) having low resistivities ($10^{-3}$ to $10^{-2}\,\Omega\,cm$). These oxides have three pronounced features. First, their valence electrons have open-shell configurations ($t_{2g}^4$ in Ru 4d and $t_{2g}^5$ in Ir 5d), which is distinctively different from the closed-shell or pseudo-closed-shell configurations in other p-type oxides (e.g., Cu $3d^{10}s^0$ in Cu oxides,[16,17] Sn $5s^2$ in SnO,[18] Rh $t_{2g}^6$ in Zn-Rh-O,[9,10,19] and Co $t_{2g}^6$ in Zn-Co-O).[11] Second, the conduction of a-La-Ru-O (semiconducting) is completely different from that of its crystalline phases (e.g., $La_3Ru_3O_{11}$ and $La_4Ru_6O_{19}$, which are both metallic),[20] while the only two known p-type a-oxides Zn-Rh-O (Refs. 9 and 10) and Zn-Co-O (Ref. 11) have crystalline counterpart phases that are also p-type semiconductors.[19,21] Third, the resistivity of solution-processed a-La-Ru-O is lower than that of the sputtered sample, whereas for common oxides (e.g., a-In-Ga-Zn-O, ITO), solution-processed films have properties inferior to those of sputtered ones. These features may provide guidelines for the search of more p-type a-oxides from solution processing. Hence, detailed understanding of the electronic structure of these materials and the mechanism underlying processing-composition-conduction correlation is of fundamental importance for future research.

These a-oxides were found during our study of printed electronics. We have focused on Ru oxides for creating a

a)Author to whom correspondence should be addressed. Electronic mail: lijw@jaist.ac.jp.

 

solution-processed electrode material. Ru oxides are technologically important and fundamentally interesting. For example, $RuO_2$ and $SrRuO_3$, both having metallic conduction, are well-known electrode materials. $Sr_2RuO_4$ is a superconductor.[22] Both $La_3Ru_3O_{11}$ and $La_4Ru_6O_{19}$ are metallic, whereas the latter is unusual for its non-Fermi-liquid behaviour.[20] $La_4Ru_2O_{10}$ is semiconducting and shows a rare full-orbital ordering transition.[23] All these Ru-oxides are crystalline; in contrast, the amorphous phases have not attracted attention. We combined Ru with La in the expectation of creating a thermally stable amorphous phase, possibly with low resistivity. As a result, we produced a series of highly interesting p-type a-oxides. Note that these oxides are not transparent; transparency has been commonly emphasized for vacuum-deposited electronic oxides because they are considered as supplementary materials to the conventional vacuum technique-based silicon that has high electrical performances but is not transparent. Nevertheless, for future vacuum-free printing of all-oxide electronics, transparency is unnecessary for most applications.

To deposit the film, solutions were prepared by dissolving metal acetates into propionic acid in ambient atmosphere through heating. Monoethanolamine was used as the chelating agent, and 1-butanol was the dilutant (see supplementary material[24] for the details of experimental methods). Next, the solutions were spin coated onto $SiO_2$/Si or $SiO_2$ glass substrates and then dried and annealed in air or oxygen. We first synthesized a-La-Ru-O and analyzed it in detail. The typical sample, annealed at 650 °C, gave a composition of $LaRu_{1.01(6)}O_{3.8(3)}C_{0.28(6)}Cl_{0.018(7)}$, where Cl was obtained as a result of impurities in the metal acetates used as starting materials. A large amount of residual carbon remained even after annealing at such a high temperature. X-ray diffraction (XRD) patterns showed no diffraction lines from the oxide after annealing up to 800 °C (Fig. 1(a) and Fig. S1 in supplementary material[24] for glancing angle XRD). Because XRD may fail to detect nanocrystals, high-resolution transmission electron microscopy (TEM) with electron diffraction (ED) was performed. It confirmed that the film is amorphous, without nanocrystals (Figs. 1(b)–1(d)). The TEM image, taken for the 650 °C-annealed sample, shows that the layers corresponding to different spin-coating cycles are clearly separated (Fig. 1(b)). This indicates that the amorphous phase is highly stable, without apparent diffusion even at such a high annealing temperature.

Atomic force microscopy (AFM) analysis (Fig. 1(e)) revealed that the film surface was smooth on the atomic scale, with a root mean square (RMS) roughness value of 0.28 nm and a peak-valley (P-V) roughness value of 2.3 nm for a scanned area of $1 \times 1\ \mu m^2$.

A significant advantage of solution processing over vacuum deposition is that the solution approach allows films to be patterned over large-area substrates simply by a printing method. The fabrication of printed electronics relies on precise pattern printing. Our solution-processed a-La-Ru-O was proven to be excellent for patterning. We patterned the film simply by direct imprinting after spin coating. As expected, the pattern shape remained after annealing, during which it shrank due to decomposition of the organic components but did not undergo any distortion or collapse because no crystallization occurred (Fig. 1(f)). This is of fundamental importance for printed nanodevices.

The film exhibits low room temperature (RT) DC electrical resistivity of 0.016–0.019 Ω cm in a wide annealing temperature range of 500–700 °C (Fig. 2(a)). At higher annealing temperatures up to 800 °C, the resistivity gradually increases, which indicates the beginning of deviation of the structure from the perfect amorphous phase because of increased diffusion rate at these temperatures. The resistivity increases by a factor of three when the annealing temperature is increased from 800 °C to 850 °C because of substantial reconstruction of the materials through crystallization. At annealing temperatures below 500 °C, the resistivity increases because of insufficient removal of organic residuals. Yet the values remain on the order of $10^{-2}$ Ω cm for annealing temperatures down to 350 °C and increase only to the order of $10^{-1}$ Ω cm for lower annealing temperatures down to 270 °C. Organic removal in thinner films is faster, leading to resistivity values lower than those of thicker films annealed under the same conditions, as seen in the 400 °C-annealed samples.

Temperature dependence of DC electrical resistivity revealed that the films were semiconducting (Fig. 2(b)). They should be degenerate semiconductors because of their low resistivity. The data were best fitted by the three-dimensional variable-range hopping model (Fig. 2(b) inset).

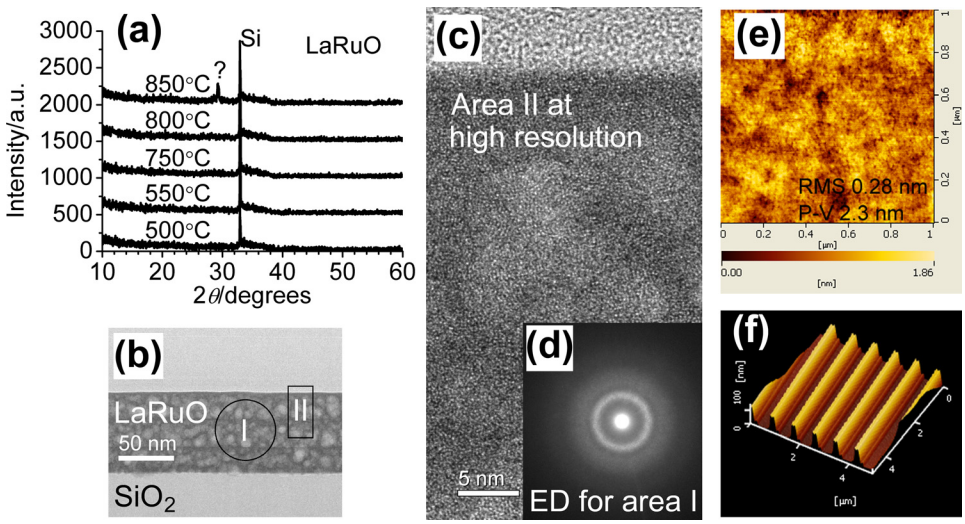


FIG. 1. Phase and morphology analyses for solution-processed a-La-Ru-O films. (a) XRD patterns for films annealed at different temperatures. (b)–(d) TEM and ED images (annealed at 650 °C). (e) AFM image of the film surface (annealed at 500 °C). (f) AFM image of an imprinted film (annealed at 550 °C).

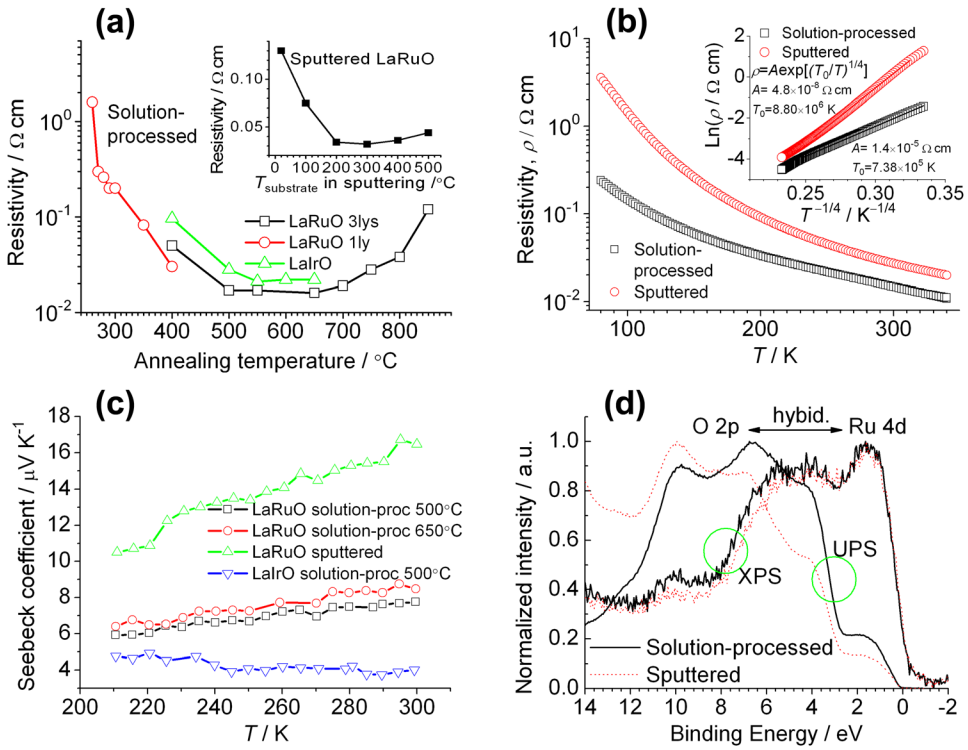


FIG. 2. (a) Room temperature DC resistivity against processing temperatures. La-Ru-O was spin coated 3 layers (3lys) or 1 layer (1ly), and La-Ir-O was spin coated 3 layers. The inset is for samples sputtered at different substrate temperatures. (b) Temperature dependence of resistivity. The inset shows fitting of the data to the three-dimensional variable-range hopping model. (c) Seebeck coefficient against measurement temperature. (d) XPS and UPS spectra for the valence band.

Positive Seebeck coefficient values (Fig. 2(c)) indicate that the conduction is p-type. The optical bandgap, determined by the Tauc plot of a UV-visible spectrum, was around 0.8 eV (Fig. S2 in supplementary material[24]).

For comparison, we also prepared a-La-Ru-O by sputtering. The optimum substrate temperature (Fig. 1(a) inset) and atmosphere were found to be ~300 °C and pure Ar, respectively. The sputtered films also showed p-type conduction by hopping transport but exhibited electrical resistivity twice (at RT) or higher (below RT), even after process optimization, than that of the solution-processed samples (Figs. 2(b) and 2(c)). A post-annealing treatment in air or oxygen did not decrease the resistivity of the sputtered sample but increased it. The sputtered sample had a composition of $LaRu0.97_{(3)}O_{3.4\text{-}(2)}H_{0.038(6)}Ar_{0.033(6)}$, where a minor amount of H may be obtained as result of impurities in the target used for sputtering, and the Ar was obtained from the gas used in sputtering. Compared to the solution-processed film, the sputtered sample contains ten times fewer impurity atoms, noticeably carbon, but the resistivity is higher. Therefore, a-La-Ru-O is preferably prepared by a simple solution process, unlike common semiconductors that show better properties for sputtered samples.

Ultraviolet photoelectron spectroscopic (UPS) and x-ray photoelectron spectroscopic (XPS) analyses for the valence band electrons in both solution-processed and sputtered samples are presented in Fig. 2(d). Both samples show the same valence electron structure. The valence band maximum (VBM) is just 0.1–0.2 eV below the Fermi level, consistent with p-type conduction. In the UPS analysis, the ionization potential was determined to be 3.8–4.0 eV, which is well inside the range for existing p-type oxides (<~5.5 eV).[25] Referring to related studies on other Ru oxides[26,27] and considering that the ratio of the ionization cross section of Ru 4d to O 2p increases at higher photon energies, the features of the UPS and XPS spectra are assigned: Ru 4d centered at 1.6 eV with hybridization with O 2p at 3–8 eV. Hybridization of metal valence orbitals with O 2p orbitals has been considered to result in delocalization of the valence band and thus to create a p-type (hole) conduction path.[17] A feature centered at 10 eV may be assigned to O 2p associated with non-network O (O not in the $RuO_6$ network) or with residual surface La-HO (Ref. 28) after cleaning by Ar ions.

The electron configuration of a-La-Ru-O is unknown at present. The high-temperature crystalline phase of the same metal composition, $La_3Ru_3O_{11}$, is metallic,[20] which is consistent with its open-shell configuration of 4d electrons (partially occupied triply degenerate $t_{2g}$ and empty doubly degenerate $e_g$).[29] The behavior of a-La-Ru-O, however, cannot be simply explained by this electron structure. The crystalline phases of Ru oxides have shown electron structures with high richness and subtle sensitivity to the compositions,[30] and the crystal field splitting model and the Hubbard band theory have been used in an effort to understand them.[29,31] The structure of our a-La-Ru-O is expected to bear some resemblance to crystalline Ru oxides but is certainly more complex. To understand a-La-Ru-O in detail, advanced theoretical analysis is necessary. This may offer instructive insight for searching other p-type a-oxides. In addition, the effect of "impurities," typically residual C and H, which may have positive contribution to p-type conduction, cannot be understood without exact theoretical modeling.

TABLE I. Variation of RT DC resistivity (Ω cm) during alternate annealing (10 min for each) in oxygen flow (0.1 MPa) and vacuum (2.0–2.5 Pa) at the indicated temperatures.

| | $O_2 \rightarrow$ vac. $\rightarrow O_2 \rightarrow$ vac. |
|---|---|
| LaRuO 650 °C | $0.017 \rightarrow 0.014 \rightarrow 0.023 \rightarrow 0.018$ |
| LaRuO 700 °C | $0.019 \rightarrow 0.60 \rightarrow 0.26 \rightarrow 0.35$ |
| LaRuO 750 °C | $0.033 \rightarrow 3.0 \times 10^5 \rightarrow 20 \rightarrow 1.2 \times 10^3$ |
| LaIrO 650 °C | $0.017 \rightarrow 630 \rightarrow 0.19 \rightarrow 6.0$ |

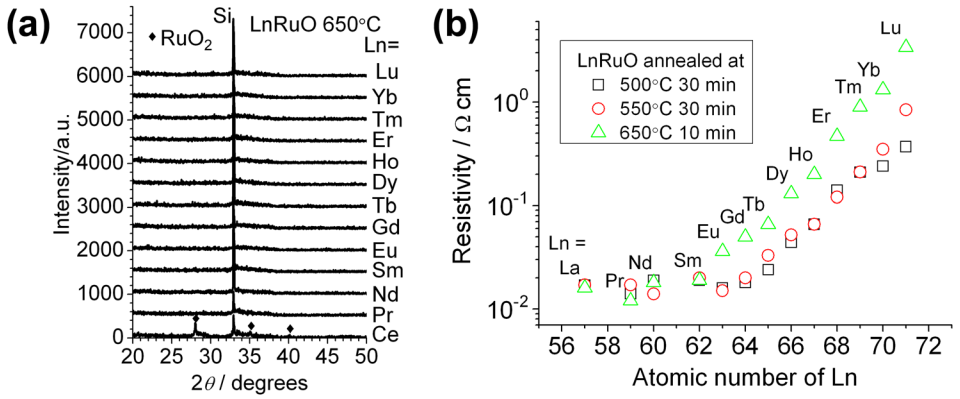


FIG. 3. (a) XRD patterns (annealed at 650 °C) and (b) room temperature DC resistivity for solution-processed Ln-Ru-O films.

As listed in Table I, the variation of RT DC resistivity during alternate annealing at 700–750 °C in oxygen and vacuum appears to support carrier generation by oxygen doping, but the results of annealing at 650 °C showed an opposite resistivity change that indicates origin of hole through mixed valence states of Ru. The annealing at 700–750 °C in vacuum may have changed the structure, as indicated by the appearance of unidentified minor peaks in the glancing angle XRD pattern for the sample annealed at 750 °C in vacuum (Fig. S1 in supplementary material[24]). The carrier generation mechanism needs more detailed study.

Replacing La by other lanthanide elements except Ce also resulted in conductive a-oxides Ln-Ru-O with similar thermal stability (Fig. 3). The resistivity increases with increasing Ln atomic number ($Z$) and changes evidently faster for $Z > 64$ (Gd), which may be more related to the influence of 4f electrons (4f subshell is more than half-filled at $Z > 64$) than to the decreasing size of Ln ions. Thus, a series of p-type a-oxides with different resistivity values from $10^{-2}$ to $10^{0}\,\Omega\,\text{cm}$ are produced.

Changing Ru to Ir, we produced a-La-Ir-O from solution processing. It was also found to be p-type with similar properties to a-La-Ru-O regarding resistivity (Figs. 2(a) and 2(c)), thermal stability, and effect of alternate annealing in vacuum and oxygen (Table I). The crystalline Ir oxides, usually having a valence state of Ir 4+ with a $5d^5$ structure, have been described in the framework of Mott physics,[32] but our a-La-Ir-O films need to be more characterized.

Another advantage of a-oxides is that the ratio of metals is allowed to vary, i.e., there is no stoichiometric metal ratio. Applying an atomic ratio of La/Ru greater or less than 1.0, we have prepared films with higher or lower resistivity values. Noticeably, we found that the amorphous phase was stable up to 750 °C for La/Ru down to 0.7, where the resistivity was lowered to below $8.0 \times 10^{-3}\,\Omega\,\text{cm}$.

In summary, using simple solution processing, we have found a series of p-type a-oxides of Ru and Ir that show low resistivity values on the order $10^{-3}\,\Omega\,\text{cm}$ and have excellent thermal stability up to 800 °C, while they can be processed below 400 °C. The film surfaces are smooth on the atomic scale, and the process allows patterning simply by direct imprinting without distortion of the pattern after annealing. These properties have high potential for use in printed electronics, e.g., as gate electrodes in n-channel oxide TFTs, and may be modified to use as a p-channel in TFTs or as an active layer in solar cells. The narrow bandgap is advantageous for light absorbing in solar cells. The electronic configurations of these a-oxides are apparently not analogous to those of known p-type oxides. This deserves theoretical investigation and suggests that more p-type a-oxides are ahead of us.

The authors thank Professor S. Katayama for helpful comments. The assistance of co-workers in measurements is acknowledged.

[1]T. Shimoda, Y. Matsuki, M. Furusawa, T. Aoki, I. Yudasaka, H. Tanaka, H. Iwasawa, D. Wang, M. Miyasaka, and Y. Takeuchi, Nature (London) **440**, 783 (2006).
[2]C. Avis and J. Jang, J. Mater. Chem. **21**, 10649 (2011).
[3]K. Jiang, J. T. Anderson, K. Hoshino, D. Li, J. F. Wager, and D. A. Keszler, Chem. Mater. **23**, 945 (2011).
[4]S. Jeong, Y.-G. Ha, J. Moon, A. Facchetti, and T. J. Marks, Adv. Mater. **22**, 1346 (2010).
[5]K. K. Banger, Y. Yamashita, K. Mori, R. L. Peterson, T. Leedham, J. Rickard, and H. Sirringhaus, Nat. Mater. **10**, 45 (2011).
[6]M.-G. Kim, M. G. Kanatzidis, A. Facchetti, and T. J. Marks, Nat. Mater. **10**, 382 (2011).
[7]M.-G. Kim, H. S. Kim, Y.-G. Ha, J. He, M. G. Kanatzidis, A. Facchetti, and T. J. Marks, J. Am. Chem. Soc. **132**, 10352 (2010).
[8]Z. L. Mensinger, J. T. Gatlin, S. T. Meyers, L. N. Zakharov, D. A. Keszler, and D. W. Johnson, Angew. Chem. Int. Ed. **47**, 9484 (2008).
[9]S. Narushima, H. Mizoguchi, K. Shimizu, K. Ueda, H. Ohta, M. Hirano, T. Kamiya, and H. Hosono, Adv. Mater. **15**, 1409 (2003).
[10]T. Kamiya, S. Narushima, H. Mizoguchi, K. Shimizu, K. Ueda, H. Ohta, M. Hirano, and H. Hosono, Adv. Funct. Mater. **15**, 968 (2005).
[11]S. H. Kim, J. A. Cianfrone, P. Sadik, K.-W. Kim, M. Ivill, and D. P. Norton, J. Appl. Phys. **107**, 103538 (2010).
[12]K. Nomura, H. Ohta, A. Takagi, T. Kamiya, M. Hirano, and H. Hosono, Nature (London) **432**, 488 (2004).
[13]K. Hayashi, S. Matsuishi, T. Kamiya, M. Hirano, and H. Hosono, Nature (London) **419**, 462 (2002).
[14]S. Matsuishi, Y. Toda, M. M. K. Hayashi, T. Kamiya, M. Hirano, I. Tanaka, and H. Hosono, Science **301**, 626 (2003).
[15]K. Nomura, H. Ohta, K. Ueda, T. Kamiya, M. Hirano, and H. Hosono, Science **300**, 1269 (2003).
[16]H. Kawazoe, M. Yasukawa, H. Hyodo, M. Kurita, H. Yanagi, and H. Hosono, Nature (London) **389**, 939–942 (1997).
[17]H. Kawazoe, H. Yanagi, K. Ueda, and H. Hosono, MRS Bull. **25**, 28 (2000).
[18]Y. Ogo, H. Hiramatsu, K. Nomura, H. Yanagi, T. Kamiya, M. Kimura, M. Hirano, and H. Hosono, Phys. Status Solidi A **206**, 2187 (2009).
[19]H. Mizoguchi, M. Hirano, S. Fujitsu, T. Takeuchi, K. Ueda, and H. Hosono, Appl. Phys. Lett. **80**, 1207 (2002).
[20]P. Khalifah, K. D. Nelson, R. Jin, Z. Q. Mao, Y. Liu, Q. Huang, X. P. A. Gao, A. P. Ramirez, and R. J. Cava, Nature (London) **411**, 669 (2001).
[21]M. Dekkers, G. Rijnders, and D. H. A. Blank, Appl. Phys. Lett. **90**, 021903 (2007).
[22]Y. Maeno, H. Hashimoto, K. Yoshida, S. Nishizaki, T. Fujita, J. G. Bednorz, and F. Lichtenberg, Nature (London) **372**, 532 (1994).
[23]P. Khalifah, R. Osborn, Q. Huang, H. W. Zandbergen, R. Jin, Y. Liu, D. Mandrus, and R. J. Cava, Science **297**, 2237 (2002).
[24]See supplementary material at http://dx.doi.org/10.1063/1.4739936 for the details of experimental methods, glancing angle XRD data, and Tauc plot for bandgap analysis.

[25]H. Hosono and T. Kamiya, Ceramics **38**, 825 (2003).
[26]J. Park, K. H. Kim, H.-J. Noh, S.-J. Oh, J.-H. Park, H.-J. Lin, and C.-T. Chen, Phys. Rev. B **69**, 165120 (2004).
[27]P. A. Cox, J. B. Goodenough, P. J. Tavener, D. Telles, and R. G. Egdell, J. Solid State Chem. **62**, 360 (1986).
[28]M. F. Sunding, K. Hadidi, S. Diplas, O. M. Løvvik, T. E. Norby, and A. E. Gunnæs, J. Electron Spectrosc. Relat. Phenom. **184**, 399 (2011).
[29]P. Khalifah and R. J. Cava, Phys. Rev. B **64**, 085111 (2001).
[30]R. J. Cava, Dalton Trans. **2004**, 2979.
[31]J. S. Lee, S. J. Moon, T. W. Noh, T. Takeda, R. Kanno, S. Yoshii, and M. Sato, Phys. Rev. B **72**, 035124 (2005).
[32]S. J. Moon, H. Jin, K. W. Kim, W. S. Choi, Y. S. Lee, J. Yu, G. Cao, A. Sumi, H. Funakubo, C. Bernhard, and T. W. Noh, Phys. Rev. Lett. **101**, 226402 (2008).